Modal decomposition of wind-tunnel fluctuations

G. Fahland*, F. Elsner, K. Weber, P. Gueib, F. Kauffmann, M. Wickberg, D. Achzehnter and J. Kriegseis †
Institute of Fluid Mechanics (ISTM), Karlsruhe Institute of Technology (KIT), Kaiserstraße 10, 76131 Karlsruhe, Germany

Low-frequency wind-tunnel fluctuations occur especially in open-jet closed-return circuit wind-tunnels. The present work addresses identification of modes within the frequency and spatial domain of these fluctuations. Experimental data is collected in a full scale tunnel and its scale model by the means of distributed, synchronized pressure measurements. Application of spectral proper orthogonal decomposition revealed the existence of multiple acoustic and convective modes. This in part confirms previous findings which were based on frequency analysis only, such as the existence of the edge-tone feedback mechanism for low speed wind-tunnels. For other idealizations, such as the wind-tunnel acting as Helmholtz resonator, no proof could be found. With this understanding improvement measures were developed, tested and improved. During this process modal decomposition led the way to fluctuation reductions of over 6dB, i.e. 50%.

Nomenclature

A	=	amplitude of oscillation
C_p	=	pressure coefficient
Cx	=	force coefficient in the x direction
D_h	=	hydraulic diameter of the nozzle
s	=	stream-wise path coordinate of the airline starting from the nozzle exit
U_∞	=	core velocity of the jet
l_{jet}	=	length of the jet measured from the nozzle exit to the first tip of any collector
POD	=	proper orthogonal decomposition
SPOD	=	spectral proper orthogonal decomposition
EF	=	edge-tone feedback
AR	=	acoustic resonance

I. Introduction

Wind tunnel design is largely a question of achieving high flow quality with the least effort. Effort in that sense means expenses which are largely driven by facility size per test object size (e.g. [1–3]). Depending on the wind-tunnel objective flow quality is judged by different properties. In many cases though, the main factor of flow quality is spatial and temporal uniformity of velocity and pressure. This can be separated into small scale velocity fluctuations (i.e. turbulence) as well as small scale pressure fluctuations, which are mostly sound waves, which in turn make up for the non-convective portion of the small scale velocity fluctuations. Typical measurement devices for these phenomena are hotwires [4] respectively microphones or piezo-electric pressure transducers [5]. At the lower end of the spectrum non-uniformities consist mostly of convective velocity fluctuations and low frequency pressure fluctuations which again are two parts of similar phenomena. While hotwire measurements can still give reasonable results the use of e.g. microphones gives false impressions of the intensity due to the high-pass filter properties of such devices which cannot pickup frequencies below 20Hz. It has to be noted though that the separation of scales is ambiguous. This is due to the fact that both terms describe similar phenomena just at different parts of the frequency spectrum. A difference lies in the underlying physics of the creation of these non-uniformities. Whilst turbulence (i.e. small scales) is basically broadband noise which can be tackled using straighteners and screens as well as large contraction ratios [1] the physics of the low-frequency fluctuations, especially in open jet wind-tunnels is more complex. It is important to note though,

*PhD Student, georg.fahland@kit.edu
†Sensior Researcher, jochen.kriegseis@kit.edu

that these large scale structures can carry significant energy and worsen the flow quality, including the turbulence level, beyond acceptable (e.g. [6–8]).

Schütz gives general considerations for test section design of open jet wind tunnels [9, ch. 13.2.4] which includes the treatment of low-frequency wind-tunnel fluctuations. Generally speaking, open jets produce significant fluctuations resulting from the instability of the free shear layer. This is an inherent feature of open jets and cannot be mitigated. For one this is a natural vortex shedding, of which the structures are convected downstream with $c_C \approx 0.65U_\infty$ with U_∞ being the jet core velocity [10]. Pressure fluctuations propagate away perpendicular to the shear layer thus creating broadband noise. At the end of the test-section those vortices impinge on the so-called collector [11, 12]. This vortex impact by itself is undesirable because again, it produces broadband noise. As a special case, the so-called Edge-Tone Feedback (EF), can occur if the produced sound-waves propagate upstream and trigger a synchronized vortex shedding [6] which results in a spectral peak of impingement events at the collector. Contrary to previous results [13] this effect also exists for low Mach number Wind tunnels [6, 14].

With the excitation resulting from the natural vortex shedding, vortex impingement as well as the EF, acoustic resonances (AR) can amplify the fluctuations significantly. Possible modes include the return circuit pipe resonance [14], the test chamber resonance [15, ch.3] or Helmholtz-Resonances although the modeling of a wind-tunnel as Helmholtz Resonator is ambiguous as suspected by [14, p.4]. The collector is situated at the interface of measurement chamber and return duct. Therefore, it plays a significant role in the creation of large-amplitude low-frequency fluctuations. Therefore, it was proposed to remodel the collector such that the vortices do not hit it straight on but at an angle, thus blurring the impingement event end its frequency in case of an existing EF loop.[16]

Another way of avoiding the impingement of large vortices on the collector is the suppression of formation of large-scale vortices in the first place [17] using vortex generators [18] or "Seifert wings" [8]. At the cost of increasing small scale turbulence in the shear layer less fluctuations in the core of the jet could be observed, presumably by the suppression of resonance effects [19]. The downside of such measures is usually a higher broadband noise generated by the shear layer [17, 18]. Recently, new passive flow control devices were reported which can mitigate this "cost" of higher broadband noise, albeit having similar effects on the low-frequency resonances: 3D vortex generators form streamwise rolers which can also suppress the formation of large-scale vortices [20]. Disturbing coherent vortex formation by active flow control at the nozzle was also reported to reduce the broadband noise compared to "Seiferth Wings" [21] while still improving on the low-frequency fluctuation similarly.

Another approach of breaking the resonance is influencing the AR eigenfrequencies, *i.e.* designing an "acoustic opening" to change the tunnel or return circuit eigenmodes [7]. So-called breather gaps can have a similar effect [3] but their location at the end of the test-section may cause excited broad band noise [22, p. 23].

Apart from excitation and eigenfrequencies, a third general approach of reducing the fluctuations is dampening. Passive dampening of such low frequencies is challenging considering the large facility footprint of broadband-low-frequency absorbers as they scale with the acoustic wave length [23]. However, so-called Helmholtz resonator devices have been proposed which can be adjusted to destructively interfere with certain frequencies thus reducing fluctuation peaks in the spectrum significantly (e.g. -8dB [24]). Given that the high level of low-frequency fluctuations is caused by few resonance interference frequencies this can lead to significant improvements. Apart from passive dampening also active systems have been proposed [14]. Yet they require extremely strong sound systems which are usually very expensive.

Overall, a lot of strategies have been proposed most of which could reduce the low-frequency fluctuations significantly, presumably by breaking resonance and feedback loops. However, the analysis was usually based on observable frequencies of low frequency fluctuations of both velocity and pressure. To the authors' knowledge no study gives a quantitative measurement of phase and amplitude distribution within the wind-tunnel. This, however, is crucial to not just have circumstantial evidence of the modes by their frequency because it could also result from a different mode within the same frequency band. Therefore, our primary objective is to analyze the fluctuations on frequency, phase and amplitude in order to proof that the convective patterns and acoustic waves actually represent the suspected modes. With this the understanding of the physical effects leading to these undesired fluctuations can be extended and the best counter measures can be identified.

Another major flow quality concern of such open jet test sections – apart from the low-frequency fluctuations – is the stream-wise pressure gradient, which ought to be low or zero at best [24, 25]. Otherwise an artificial drag or thrust force, called horizontal buoyancy, acts on the test objects [26, p. 24]. Potentially the collector design – which the literature review identified as a major contributor to the fluctuations – plays a huge role for this stream-wise pressure gradient as well [27, p. 40]. Leveraging on this correlation, a secondary objective for the flow quality improvement measures investigated in this study is the reduction of the stream-wise pressure gradient.

II. Methodology

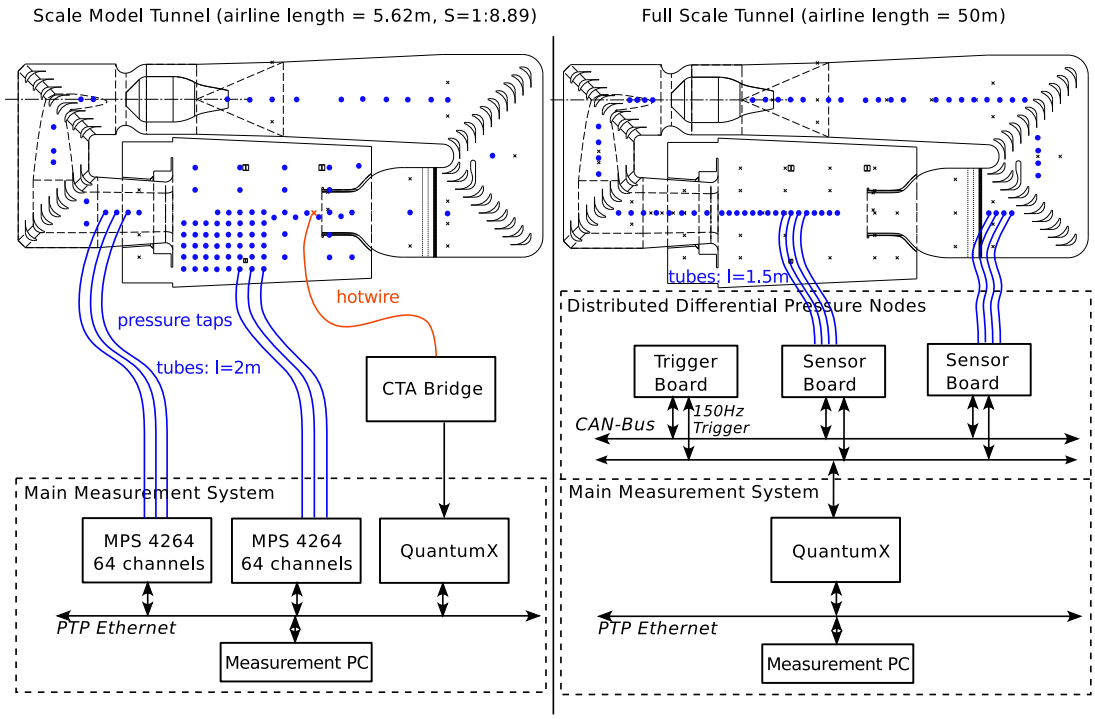

Fig. 1 Schematic of data flow and measurement hardware for scale model tunnel (left) and full scale tunnel (right).

The investigations are based around distributed, time-resolved pressure measurements. This enables a correlation analysis on the fluctuations within the whole tunnel. This supports the objective of investigating phase and amplitude of the low-frequency fluctuations formulated above, thus allowing a better interpretation of important modes than plain frequency measurements can do.

In order to not disrupt the wind-tunnel service and enable fast iterations on improvement measures a scale model wind-tunnel was designed [28]. This is a common and successful means of investigating wind-tunnel improvement measures despite different operating Reynolds Numbers Re [6, 8, 11, 25, 29–31].

A sketch of each tunnel is provided in figure 1 which additionally shows the applied measurement schematics. At the scale model tunnel the *Scanivalve MPS 4264* transducers are used with a sampling rate of 850Hz. This means the sensor stands at a centralized position within 2m tubing of each pressure tap. For the full scale tunnel a centralized sensor position is not feasible due to long tubing acting as low pass filter. Therefore 16 sensor boards with 4 *Honeywell ABP2 +-5iH20* each are placed within 1.5m tubing length of the corresponding pressure taps. Signal synchronization is achieved digitally: A trigger signal is broadcast via CAN-bus at a rate of 150Hz. Each sensor board performs a measurement upon receiving the trigger message and stores the result internally. Afterwards, the sensor boards send their result one after another on the CAN bus which is recorded by a QuantumX module. The QuantumX module stores the received data in virtual channels for each single *Honeywell ABP2* sensor. These virtual channels get over-sampled at a rate of 600Hz which ensures that every single sensor reading is recorded with 4 samples each. This avoids dropping data points which could originate from the CAN-bus not operating in sync with the QuantumX. The maximum sync error of the sensor data equals the time-delay between the result CAN-telegram of the first and the last sensor board to send on the CAN-bus. This is approximately 3ms. The digital data is down-sampled to 150Hz again prior to further data processing.

In a first step, comparison to literature should be achieved. This means comparing the characteristic amplitude magnitudes of the wind-tunnel as a whole for varying jet core velocities U_∞. For this purpose the Welch method was used. It is based on averaging the magnitude of multiple Discrete Fourrier Transforms performed with Fast Fourrier (FFT) algorithms [32, p. 19]. For further processing the magnitude of these spectra — which represents the fluctuation

pressure $\tilde{p_M}$ of each frequency bin — is transformed to sound pressure level (SPL) in decibel without filtering ($dB(Z)$). Note that the reference pressure is defined to be $p_0 = 20\mu Pa$. The sensor noise spectrum based on the ambient pressure fluctution $\tilde{p_A}$ is subtracted from each measurement. This means the resulting spectra show the sound pressure level above background and sensor noise.

$$\mathrm{SPL}_{dB(Z)} = 20\log_{10}\left(\frac{\tilde{p_M}}{p_0}\right) - 20\log_{10}\left(\frac{\tilde{p_A}}{p_0}\right) \tag{1}$$

Finally, all results below the threshold of $\mathrm{SPL}_{dB(Z)} < \frac{p_M}{p_A} = 2 \approx 6dB(Z)$ are neglected. This highlights the spectral regions where significant fluctuation measurements were recorded.

Although a fourrier transform can give the phase angle, application of the Welch method erases this information. A Proper Orthogonal Decomposition (POD) enables retrieving phase as well as amplitude. By correlating multiple – this gives the spatial information – synchronized time-series, the modes with the highest energy can be identified as the ones with the largest eigenvectors of the cross-correlation matrix [33]. Due to the nature of correlating events the POD does not give any frequency information.

The Spectral Proper Orthogonal Decomposition (SPOD) introduces the frequency information to the POD by performing a FFT first and a POD on all the FFT bins of similar frequency of the separate time-series [34, 35]. This expands the modal results by the dimension of the frequency which means the result space can be indexed by frequency, tunnel velocity and mode number. This results in a vast amount of modes to be analyzed.

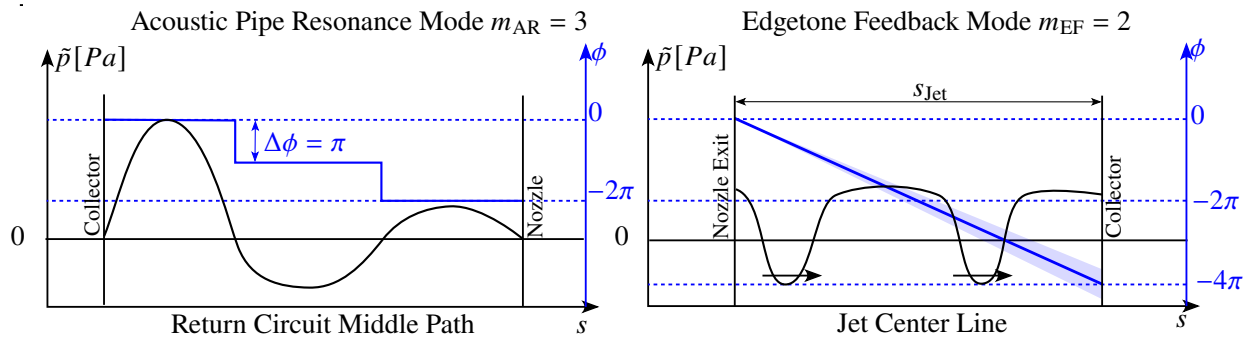

Fig. 2 Identification Criteria for AR modes (left) and EF modes (right). Adapted from [36]

One way to treat this large data pile is to check for the significance of each frequency-tunnel-velocity bin. Elsner [37] proposed the application of the so-called Gini-Coefficient [38, Appendix 2], which was initially introduced as measure conceived to quantify the inequality in income across an economy. It allows a statement about how important it is to consider more than just the first SPOD mode for a given tunnel velocity and frequency. The higher the Gini-Coefficient, the more the fluctuation is dominated by few or even just one mode.

An alternative approach is to find formal modal criteria which can be applied to each SPOD-mode. This way AR such as the pipe resonance and convective modes such as the EF can be identified by there spatial amplitude and phase distribution in a quantitative manner [36]. Figure 2 left shows an idealized way of identifying the acoustic pipe resonance of the return circuit. Phase-jumps by $\Delta\phi = \pi$ indicate a wave node. The number of wave nodes $n_{\Delta\phi}$ found *in between* the tube ends gives the information about the acoustic mode number m_{AR}. Depending on whether the tunnel ends are treated as closed or open tube ends the mode m relates to the number of pressure nodes $n_{\Delta\phi}$ as follows:

$$m_{\mathrm{AR}} = \begin{cases} n_{\Delta\phi} & \text{Both duct ends act as closed tube end} \\ n_{\Delta\phi} + 1 & \text{Both duct ends act as open tube end} \\ 2n_{\Delta\phi} + 1 & \text{One of the duct ends act as open tube end, theother closed} \end{cases} \tag{2}$$

This is a necessary criterion. Due to unavoidable noise and a rather sparse probe point distribution it is possible to miss or mistakenly identify phase jumps. Therefore, the distance of the identified wave nodes Δs is calculated. It has to match half the theoretical wave length λ. For a positive match the margin of $\Delta s_M = \pm\frac{\lambda}{10}$ has to be met. This acts as sufficient criteria to identify an AR mode.

Similarly, the EF modes can be identified by the propagation of vortices within the measurement chamber (figure 2 right), which results in a linearly falling phase ϕ because the coherent structures are convected at a somewhat constant

speed. If the vortices are correlated in time and triggered by previous impingement events, the phenomenon of the edge-tone feedback [6, p. 3] is present.

$$f_{\mathrm{EF}} = \frac{1}{\underbrace{\frac{1}{m_{\mathrm{EF}}}\underbrace{\frac{l_{\mathrm{Jet}}}{0.65U_\infty}}_{T_f} + \underbrace{\frac{l_{\mathrm{Jet}}}{c-u}}_{T_b}}_{T_{ff}}} \tag{3}$$

The mode of the edgetone feedback m_{EF} corresponds to the number of vortexes present in between nozzle and collector. The eigenfrequency f_{EF} is calculated from the inverse of the sum of the forward feedback interval T_{ff} and backward time interval T_b. T_{ff} is calculated with T_f divided by the number of vortexes present m_{EF}. The forward time interval T_f describes the time a vortex needs to convect from the nozzle to its impact at the collector. The backward time interval is the time a sound wave needs to travel from the impact event backwards (upstream) to the nozzle. Note, that the common assumption of the backward propagation time being negligible is not at all justified as will be shown later. A quantitative criterion of the EF as depicted in figure 2 can be formulated based on the phase slope within the measurement region. Because EF describes the situation where vortex shedding at the nozzle is triggered by previous vortexes, the feedback loop has to form a multiple of 2π in the phase signal. With this, the phase at the location of the collector $\phi(x = l_{\mathrm{Jet}})$ can be calculated from the ratios of forward and backward propagation time interval

$$\phi(x = l_{\mathrm{Jet}}) = \underbrace{-2\pi \cdot m_{\mathrm{EF}}}_{\text{Closed Phase loop}} \cdot \frac{T_f}{T_f + T_b} \tag{4}$$

$$\frac{\partial \phi(x)}{\partial x} = -2\pi \cdot m_{\mathrm{EF}} \cdot \frac{T_f}{T_f + T_b} \cdot \frac{1}{l_{\mathrm{Jet}}} \tag{5}$$

If the phase slope of the experiment is within a margin of $e = \pm 5\% \frac{2\pi}{l_{\mathrm{Jet}}}$ of the ideal EF phase slope of equation 5 the corresponding EF-mode is identified. This is both necessary and sufficient criterion of the EF modes.

III. Results

A. Baseline Analysis

Figure 3 gives a general overview over the occurrence of fluctuations at different wind-tunnel speeds for the present wind-tunnel. For the full scale tunnel acoustic resonances are observable (vertical patterns) as well as some anomalies, which match the theoretical EF eigenfrequencies quite accurately. Clearly, the idealization curves of edge tone feedback which result from equation 3, are superior to the simplified version with the common assumption that $T_b = 0$. This assumption would lead to linear theoretical EF lines. Such spectra can be obtained from single point measurements at a representative position within the tunnel, e.g. a typical test object position. They can provide circumstantial evidence about relevant tunnel fluctuation modes. For the scale model tunnel the patterns are less pronounced. This is to be expected, because occurring frequencies scale with the inverse geometric scale. Meanwhile the tubing length of the scale model tunnel pressure taps is slightly higher, which results in a stronger low pass filter effect compared the full scale tunnel. Furthermore, the pressure tap diameter of the full scale tunnel and the scale model tunnel are identical in absolute size ($d_H = 1mm$), which results in a much larger dimensionless hole diameter for scale model tunnel. In combination these effects result in a higher broad band noise for the scale model tunnel and less pronounced fluctuation peaks of the spectrum. Identifying AR and EF modes from figure 3 alone is ambiguous even for the full scale tunnel though. This is due to ambiguity in identifying, which geometry features represent the relevant ones for the resonances. Therefore, it is impossible to know the exact properties of the modes, e.g. the information if the nozzle of the wind-tunnel acts as a closed or opened tube end. Note, that the AR eigenfrequencies are added to the plot anticipating the results from SPOD shown later of how to treat the duct ends properly. For the full scale tunnel figure 3 suggests an acoustic resonance at $f_e = 11.3 \pm 0.5Hz$, which could be identified as third AR Mode of the whole tunnel path with both ends treated as open tube ends. Alternatively, it would also be possible to identify it as fifth mode of the return duct treating the nozzle as a closed tube end based on the frequency information only.

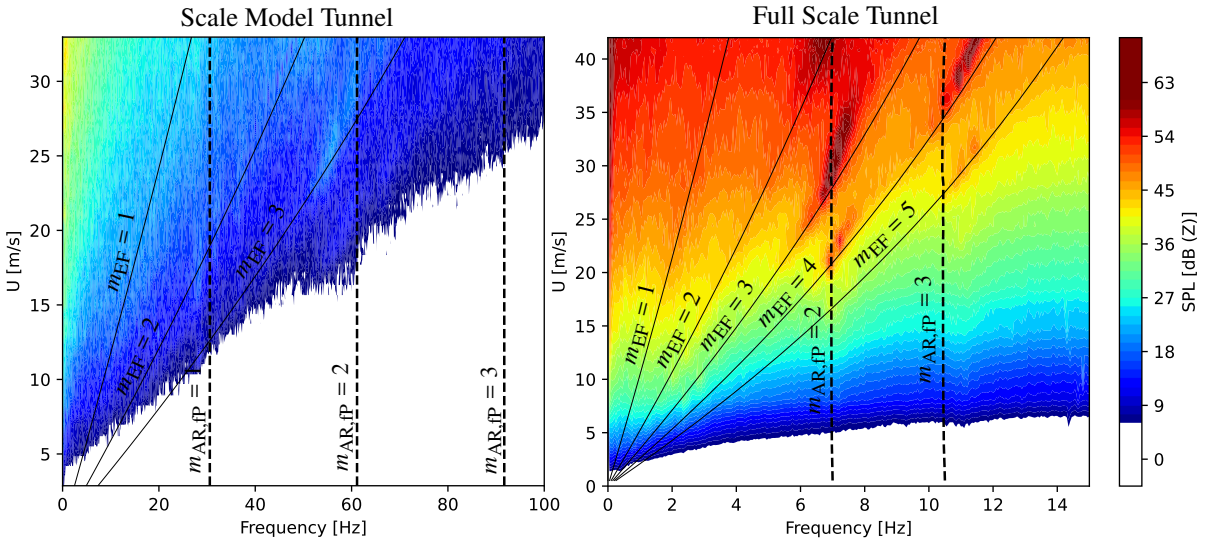

Fig. 3 Welch spectra of the scale model tunnel (left) and the full scale tunnel (right). Vertical lines indicate theoretical AR modes of the full tunnel path, sloped lines indicate theoretical edge-tone feedback.

The Proper Orthogonal Decomposition (POD) or the Spectral Proper Orthogonal Decomposition (SPOD) provide phase and amplitude information in order to check whether these suspected modes are identified correctly. Prior to checking SPOD results it has to be confirmed though how many SPOD modes make up for majority of fluctuation intensity. The Gini coefficient enables such a data reduction to fewer or single modes if it resumes values close to one. Figure 4 shows the Gini result of the model scale tunnel. In contrast to figure 3 the spectral patterns appear more pronounced also for the scale model tunnel. This is due to the fact that at intensity peaks the resonance modes stand out from the broadband noise in terms of their portion of the general fluctuation level. This means, the Gini-Spectrum in figure 4 improves data analysis in two ways: It improves the visibility of resonance regions of a spectrum especially for data with higher broadband noise levels. Additionally it enables a data reduction to representative SPOD modes. This directs the focus to operating points where resonances outweigh broadband noise, especially if the data acquisition suffers from such noise. Note, that the linear curves of the simplified EF formula ($T_b = 0$) do not match the spectral patterns which appear slightly curved, especially for higher EF modes.

For the full scale tunnel the probe grid density on the duct center line is higher than in the scale model tunnel (see

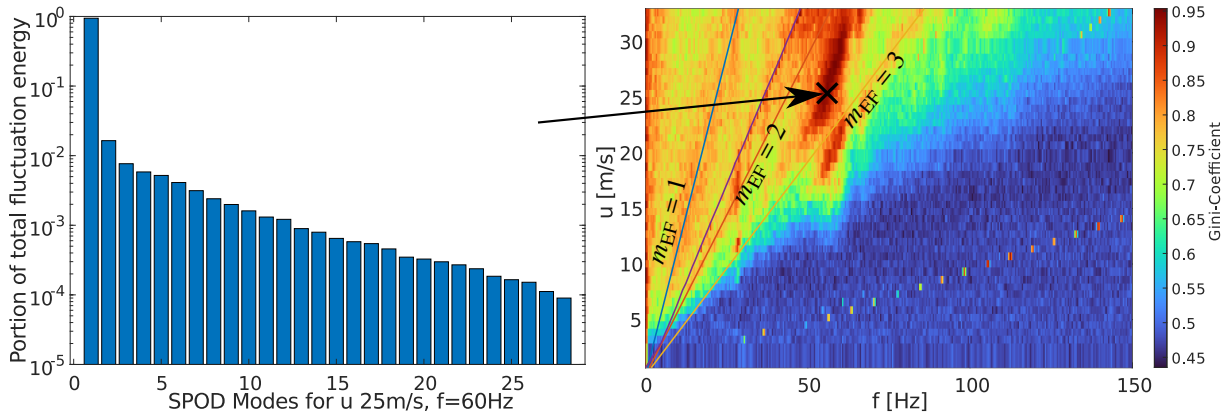

Fig. 4 Plot of the Gini-Coefficient, which composes of the energy distribution of SPOD modes for each frequency bin of each tunnel velocity. Scale model tunnel data, adapted from [37].

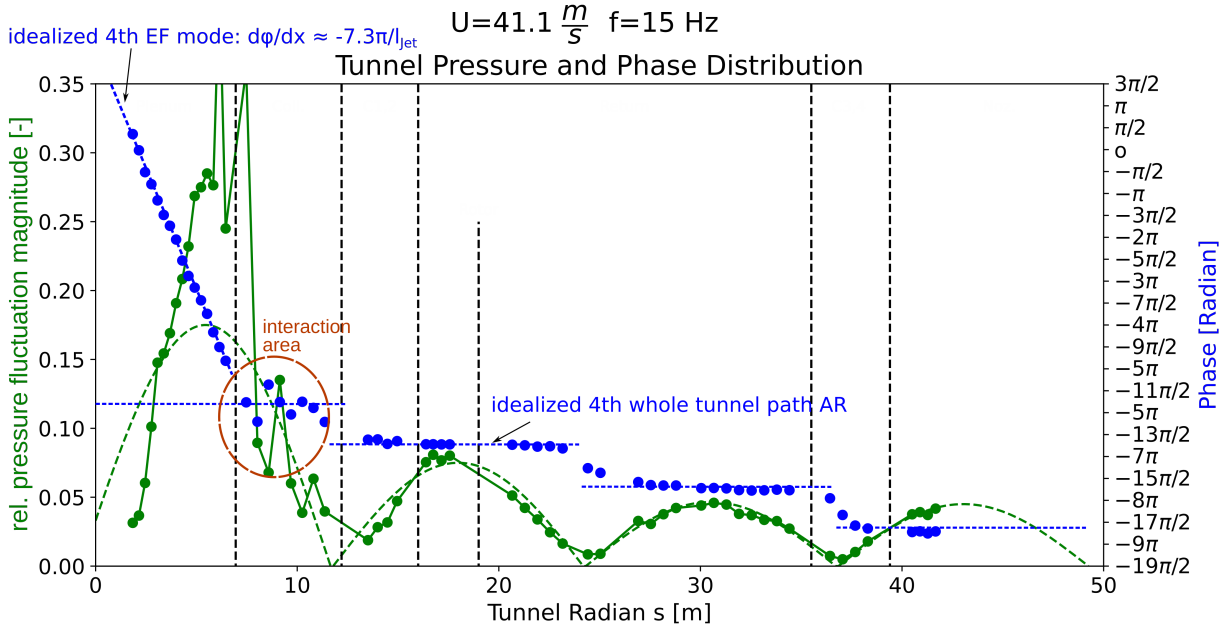

Fig. 5 Phase and amplitude throughout the tunnel for the first SPOD mode at $U_\infty = 41.1 m/s$ and $f = 15$Hz. Dashed lines show the idealized distribution of the fourth AR of the whole tunnel path and the phase slope of the fourth EF mode. Full scale tunnel data, adapted from [36, p. 64].

figure 1). For the full scale tunnel it is therefore possible to perform a phase analysis as depicted in figure 2 completely automated on the whole data set and still identify even complex modes such as the one depicted in figure 5. The 4th acoustic resonance mode of the whole tunnel path is identified and the 4th edge tone feedback mode represents the convective pattern in the measurement chamber. Both phase jumps and phase slope very clearly represent the theoretical idea formulated in figure 2. The decrease in amplitude with tunnel coordinate follows the increase in duct cross-section.

Similarly, such analysis proofs that the third full tunnel path AR is indeed the best description of the spatial fluctuation distribution both in phase and amplitude of the first SPOD mode at 10.2 Hz of the full scale tunnel (figure 3). The ambiguity about this identification raised earlier is therefore obsolete. A similar operation on the scale model tunnel confirms a similar pattern for the corresponding spectral hot spot.

Performing the aforementioned analysis on multiple SPOD modes for each tunnel velocity results in figure 6 where identified EF modes are depicted as circles and AR modes are depicted as triangles. The three different sizes of the symbols represent if the first, second or third SPOD mode of the corresponding bin defined the result. Two things can be read from this. For one, the EF is almost always present. The convection speed of the natural vortex formation almost always locks in creating these coherent, frequent structures. Therefore, the spread in convection speed is quite high. However, on average the literature value of the convection speed matching $c_C \approx 0.65 U_\infty$ [6] is met almost perfectly.

Secondly, the interaction of the EF with the AR is not always constructive. For the AR of the full tunnel path – hence an acoustic standing wave also present in the measurement chamber – the EF does not occur at the spectrum hotspots. This interaction can be explained by the dominance of the AR mode over the amplitude of the sound-wave feedback of the EF. Vice versa, at the same frequency but higher velocity and strong edge-tone feed-back occurrence the AR has rather low intensity. Therefore, the vortex shedding is rather triggered to be in-phase with the AR wave. Yet, at the fourth mode of the return duct AR the acoustic standing wave and the fourth EF mode are present in the same (the first) SPOD-mode also (figure 5). Despite a somewhat noisy interaction region inside the collector the EF is in phase with the AR. Hence, the acoustic standing wave can constructively interfere with the vortex triggering of the EF.

All spectral plots presented so far showed the tunnel speed and the frequencies with corresponding dimensions m/s and Hz. The identification of AR and EF modes and the similarity across scales enables another step in terms of generalization. It is possible to describe the tunnel speed as multiples from convective patterns such as EF or natural

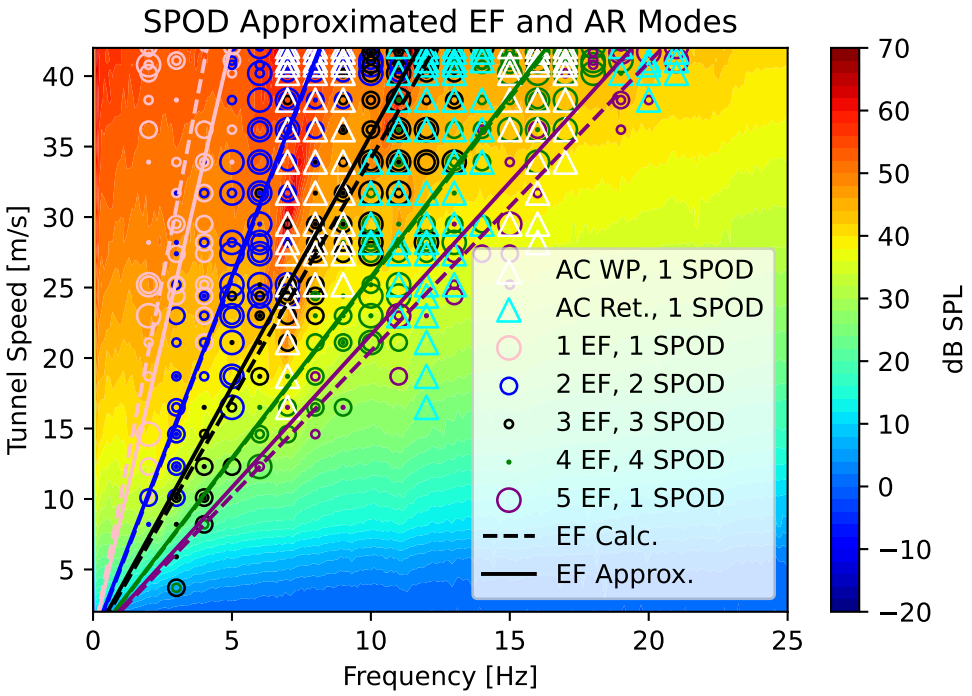

Fig. 6 Fluctuation Magnitude for different tunnel speeds and frequencies (background color plot). Identified EF-modes in circles, AR-modes in triangles. From [36, p. 64]

vortex shedding and the fluctuation frequency as multiples from acoustic eigenfrequencies. In figure 7 this is done for both the scale model tunnel and the full scale tunnel. The better signal to noise ratio of the full scale tunnel experiments allows for a larger portion of the resonance mode chart to be displayed. Yet for both scale model tunnel and full scale tunnel the benefit of such a data representation becomes clearer: No matter the tunnel scale — and presumably other geometric properties — the spectral intensity hot spots are close to natural multiples of modal numbers. Therefore, this data representation allows for the comparison of spectra across scales and also across tunnel modifications no matter if

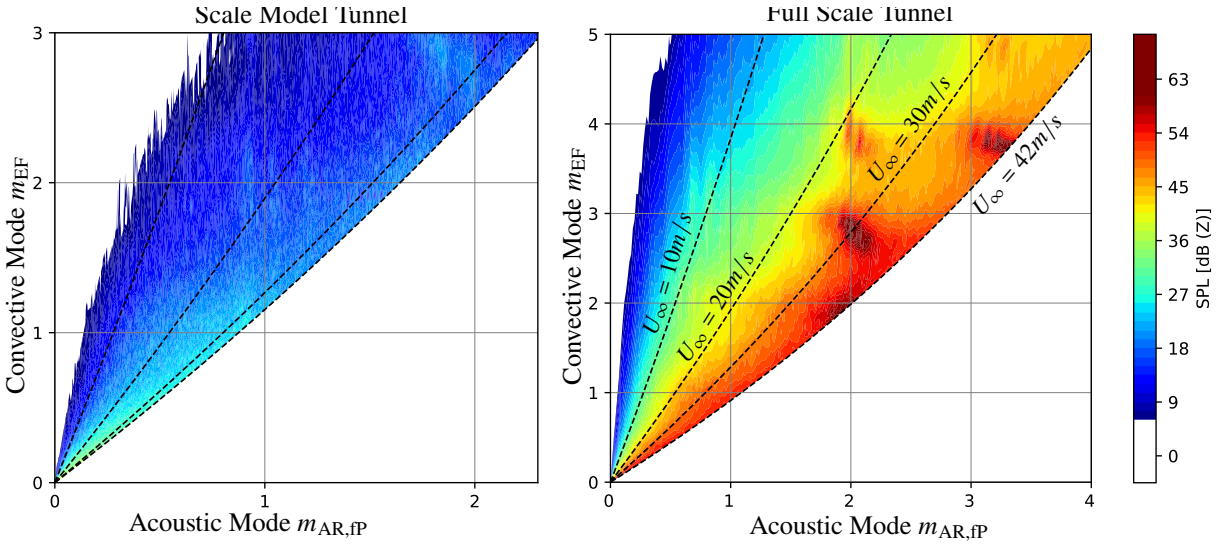

Fig. 7 Resonance mode chart for the scale model tunnel (left) and the full scale tunnel (right).

geometric properties such as nozzle diameter or test section length are changed. This enables a conclusion if a tunnel modification actually improved the tunnel quality or just shifted intensity peaks.

B. Preliminary Conclusions

All analysis of the existing wind-tunnel both in the full scale tunnel and the scale model deliver similar results: EF can definitely be present in low-speed wind-tunnels as concluded by frequency analyses of Rennie [6] and contrary to Lepicovsky [13]. For the present wind tunnel it is even the dominant fluctuation excitation mechanism. However, it is important not to apply the common simplification of the back-propagation time being negligible. This misleads the EF identification, especially for higher EF modes even at tunnel speeds far below $Ma = 0.3$. Only for few parts of the spectrum AR sound waves dominate the vortex shedding. Furthermore, no evidence could be found that fluctuation patterns within the wind-tunnel match those of a Helmholtz resonator. Identification of this effect in previous studies based solely on frequency analyses where most likely a result of the ambiguous interpretation of geometric quantities used to calculate the theoretical Helmholtz resonator frequencies. This ambiguity and the subsequent uncertainty of the resonance frequencies which can lead to false interpretation was already suspected by Wickern *et al.*[14]. It has to be noted though that this conclusion is limited to the present wind-tunnel geometry – though at two scales – and has to be generalized by conducting similar analyses in different facilities. The present study underlines that in order to avoid misled conclusions SPOD should be employed to gain spatial phase and amplitude information in addition to frequency analyses.

C. Improvement Measures

With the knowledge of spectrum hotspots and dominant modes flow quality enhancement measures can be developed at the scale model tunnel as intended. So far, four studies have been performed. These investigate common modifications

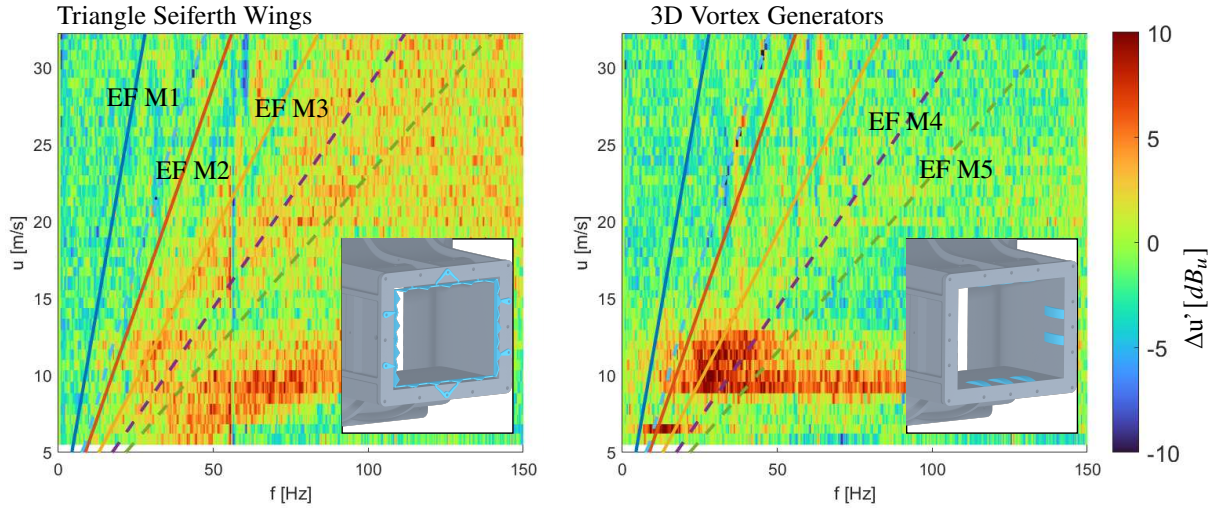

Fig. 8 Changes in logarithmic velocity fluctuations measured via hotwire of triangle-shaped "Seiferth Wings" (left) and 3D Vortex Generators (right) in comparison with the baseline tunnel configuration (plain nozzle). Plot definition: [spectrum(variation) − spectrum(baseline)]. Scale model tunnel data, adapted from [39]

at the nozzle and the collector, hence the excitation part of the resonances. Kauffmann [39] tested the effect of multiple vortex generators and "Seiferth wings" configurations. They are known to suppress coherent donut-shaped vortex formation as it is present for the EF by creating streamwise vortices. The most effective configurations of the present study in terms of reducing the fluctuation are shown in figure 8. As for the "Seiferth Wings" the variant of triangle shapes exceed rectangular shapes both in terms of less low-frequency fluctuations as well as lower penalty of broad-band noise in higher frequencies. Even better are the 3D Vortex generators as they cause almost no additional high frequency, broadband noise. Meanwhile their effect of suppressing low-frequency fluctuations is only slightly less compared to the "Seiferth wings". Contrary to Jin [18] the configuration with centered vortex generators is better than that of

vortex generators in the corners of the nozzle for the present wind tunnel. The observations are in line with theoretical properties of sharp-edged edges in turbulent flow [40]: Sharper edges like common ”Seiferth wings” have a higher theoretical sound emission. In contrast, bluff edges act as a less strong source of sound pressure waves upon vortex detachment.

In terms of collector design Wickberg [41] proposed the ”teeth collector”, a more general approach to the angled collector proposed by Lacey [16] for 3/4 automotive test sections. The general idea of such a collector design is to change vortex impact not to be a single event but stretched in streamwise direction and therefore over time in order to attenuate the EF mechanism. Wickberg [41] showed that this concept works in principle. Rufer [42] achieved significant flow quality enhancement with an improved design (fig. 9). In the regions of EF fluctuation intensity reductions are observable which have no corresponding fluctuation enhancement. Such excitation is observable for the funnel collector type in figure 9 on the right. Although sloped improvement patterns are observable, there is also fluctuation enhancement observable at the same frequency but different tunnel velocities.

Despite the successful suppression of the EF mechanism and overall fluctuation reduction by the teeth collector, the improved funnel collector operates even superior. This plays out as much less broadband noise of this collector design compared to the teeth collector. The higher broadband noise of the teeth collector is suspected to be caused by the sharp edge of the teeth which have a higher theoretical sound emission coefficient than a bluff edge [40] similar to the effect of the ”Seiferth wings”. Presumably, future teeth collector designs should therefore incorporate bluff edges perpendicular to the main flow direction and zick-zack shape in main flow direction only.

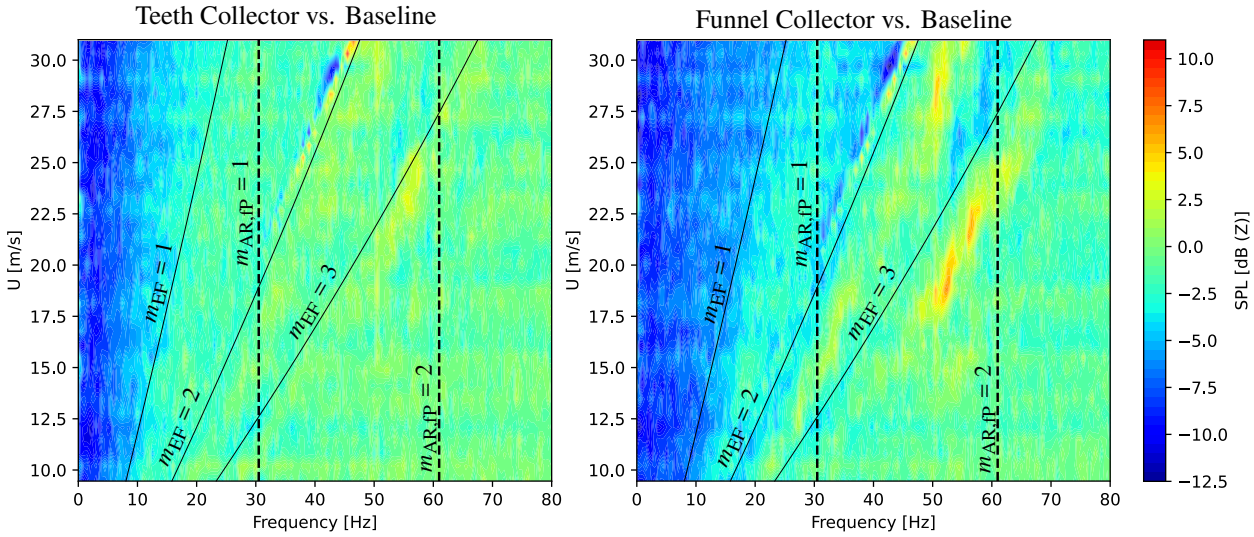

Fig. 9 Improved collector designs. The teeth-collector (left) and a classical funnel collector with overly large inflow cross section, adapted from [42]

Despite the fact that the improved funnel collector design investigated here is not as successful in suppressing the EF as the teeth collector, its broad-band properties render it superior to the investigated teeth collector. This is also due to the fact that an isolated intensity peak is less of a problem compared to multiple broadband peaks. In terms of treating isolated peaks another advantage of the spatial and frequency modal decomposition can be leveraged: With the knowledge of dominant modes for the problematic frequencies it is possible to evaluate exact positions of the pressure wave nodes and amplitude peaks in the duct. This enables tailored placement of damping devices such as Helmholtz resonator inlets.

IV. Conclusions

Wind-tunnel fluctuations of an open-jet, closed return circuit wind-tunnel were investigated experimentally in order to prepare for tailored improvement measures of such wind-tunnels. Previous studies throughout the community of automotive wind-tunnel designers suspected a special case of vortex shedding of the free jet named edge-tone feedback to be responsible for frequency hot-spots at least partially. This was concluded from the dependency of such hot-spots in the spectrum from wind-tunnel velocity, which also fell within the range of realistic edge-tone feedback modes. It

remained unclear, however, whether or not the identified modes were a correct representation of the phase and amplitude distribution throughout the wind-tunnel.

This lack of information was gained in the present investigation by employing SPOD analysis on distributed, time-resolved, synchronized pressure measurements. The obtained results and subsequently processed data revealed sufficient information to evaluate, whether the modal identifications based on theoretical eigenfrequency calculation such as pipe resonances or edge-tone feedback actually reflect a certain fluctuation pattern of the wind tunnel. In terms of mode dominance a data reduction of the decomposed modes has been found to be required, so as to quantify the intensity distribution among different modes within one frequency and tunnel-velocity bin. The Gini-Coefficient is one possible quantity, which was successfully employed for this purpose. All of these data processing steps reveal similar behavior over the investigated span of wind tunnel scale of approximately one order of magnitude. Convective mode numbers proof to be meaningful in order to translate tunnel velocity to a dimensionless number. Similarly, acoustic eigenfrequencies can be employed to translate spectrum frequencies to dimensionless quantities.

In conclusion from the above-elaborated summary of insights, the introduced processing framework is suitable to characterize a wind-tunnel design in terms of fluctuation patterns, which are common – especially, but not exclusively – for free-jet tunnel configurations. For the tunnel at hand, consequently, the framework enabled tailored tunnel design such as improved duct or nozzle geometries as well as optimized damping device placement of both passive and active damping devices. On the grounds of the achieved insights and tunnel modifications, even further improvements of the present wind-tunnel design seem possible despite a sizeable decrease of low frequency fluctuations, which also improves the turbulence level greatly.

References

[1] Bradshaw, P., and Pankhurst, R., "The design of low-speed wind tunnels," *Progress in Aerospace Sciences*, Vol. 5, 1964, pp. 1–69. https://doi.org/10.1016/0376-0421(64)90003-X, URL https://linkinghub.elsevier.com/retrieve/pii/037604216490003X.

[2] Börger, G.-G., "Optimierung von Windkanaldüsen für den Unterschallbereich," PhD Thesis, Universität Bochum, Bochum, 1973.

[3] Schwartekopp, B., "The New Daimler Automotive Wind Tunnel: Design and Aerodynamic Features," *Internationales Stuttgarter Symposium*, FKFS, Stuttgart, 2010.

[4] Örlü, R., and Vinuesa, R., "Thermal anemometry," *Experimental Aerodynamics*, CRC Press Taylor & Francis Group, Boca Raton, 2017, 1st ed., pp. 393–428.

[5] Owen, F. K., and Owen, A. K., "Measurement and assessment of wind tunnel flow quality," *Progress in Aerospace Sciences*, Vol. 44, No. 5, 2008, pp. 315–348. https://doi.org/10.1016/j.paerosci.2008.04.002, URL https://linkinghub.elsevier.com/retrieve/pii/S0376042108000286.

[6] Rennie, M., Kim, M.-S., Lee, J.-H., and Kee, J.-D., "Suppression of Open-Jet Pressure Fluctuations in the Hyundai Aeroacoustic Wind Tunnel," SAE International, 2004, pp. 2004–01–0803. https://doi.org/10.4271/2004-01-0803, URL https://www.sae.org/content/2004-01-0803/.

[7] Kudo, T., Komatsu, Y., Maeda, K., and Nishimura, M., "Techniques for Reducing Low-Frequency Fluctuations in Aeroacoustic Wind Tunnels," *JEE*, Vol. 4, No. 2, 2009, pp. 289–301. https://doi.org/10.1299/jee.4.289, URL http://www.jstage.jst.go.jp/article/jee/4/2/4_2_289/_article.

[8] Arnette, S. A., Buchanan, T. D., and Zabat, M., "On Low-Frequency Pressure Pulsations and Static Pressure Distribution in Open Jet Automotive Wind Tunnels," SAE International, 1999, pp. 1999–01–0813. https://doi.org/10.4271/1999-01-0813, URL https://www.sae.org/content/1999-01-0813/.

[9] Schütz, T. (ed.), *Hucho - Aerodynamik des Automobils*, Springer Fachmedien Wiesbaden, Wiesbaden, 2013. https://doi.org/10.1007/978-3-8348-2316-8, URL http://link.springer.com/10.1007/978-3-8348-2316-8.

[10] Ahuja, K., Massey, K., D'Agostino, M., Ahuja, K., Massey, K., and D'Agostino, M., "Flow/acoustic interactions in open-jet wind tunnels," *3rd AIAA/CEAS Aeroacoustics Conference*, American Institute of Aeronautics and Astronautics, Atlanta,GA,U.S.A., 1997. https://doi.org/10.2514/6.1997-1691, URL https://arc.aiaa.org/doi/10.2514/6.1997-1691.

[11] Wiedemann, J., Wickern, G., Ewald, B., and Mattern, C., "Audi Aero-Acoustic Wind Tunnel," SAE International, 1993. https://doi.org/10.4271/930300, URL https://www.sae.org/content/930300/.

[12] Barlow, J. B., Rae, W. H., Pope, A., and Pope, A., *Low-speed wind tunnel testing*, 3rd ed., Wiley, New York, 1999.

[13] Lepicovsky, J., and Ahuja, K. K., "Experimental results on edge-tone oscillations in high-speed subsonic jets," *AIAA Journal*, Vol. 23, No. 10, 1985, pp. 1463–1468. https://doi.org/10.2514/3.9111, URL https://arc.aiaa.org/doi/10.2514/3.9111.

[14] Wickern, G., Von Heesen, W., and Wallmann, S., "Wind Tunnel Pulsations and their Active Suppression," SAE International, 2000, pp. 2000–01–0869. https://doi.org/10.4271/2000-01-0869, URL https://www.sae.org/content/2000-01-0869/.

[15] Schönleber, C., *Untersuchung von transienten Interferenzeffekten in einem Freistrahlwindkanal für Automobile*, Wissenschaftliche Reihe Fahrzeugtechnik Universität Stuttgart, Springer Vieweg, Wiesbaden [Heidelberg], 2021.

[16] Lacey, J., "A Study of the Pulsations in a 3/4 Open Jet Wind Tunnel," SAE International, 2002, pp. 2002–01–0251. https://doi.org/10.4271/2002-01-0251, URL https://www.sae.org/content/2002-01-0251/.

[17] Sellers, W. L., Applin, Z. T., Molloy, J. K., and Gentry, G. L. J., "Effect of jet exit vanes on flow pulsations in an open-jet wind tunnel," Technical Memorandum 86299, NASA, 1985.

[18] Jin, L., Sun, H., Jiang, Y., Liang, Y., and Zhang, J., "Suppression of low-frequency pressure pulsations in an open jet wind tunnel by corner vortex generators," *AIP Advances*, Vol. 11, No. 6, 2021, p. 065306. https://doi.org/10.1063/5.0056092, URL https://aip.scitation.org/doi/10.1063/5.0056092.

[19] Papenfuss, H. D., Holzdeppe, D., Lorenz-Meyer, W., Roukavets, V. P., and Filatov, A. P., "H. D. Papenfuss u. a. „Lowering the turbulence level in an open-jet wind tunnel by novel adjustable jet-exit vanes". In: Agard Conference Proceedings 585, Aerodynamics of Wind Tunnel Circuits and their Components (1997), S. 316–319," *Agard Conference Proceedings*, Vol. 585, AGARD, Moscow, Russia, 1996, pp. 25B–x.

[20] Blumrich, R., Widdecke, N., Wiedemann, J., Michelbach, A., Wittmeier, F., and Beland, O., "New FKFS Technology at the Full-Scale Aeroacoustic Wind Tunnel of University of Stuttgart," *SAE Int. J. Passeng. Cars - Mech. Syst.*, Vol. 8, No. 1, 2015, pp. 294–305. https://doi.org/10.4271/2015-01-1557, URL https://www.sae.org/content/2015-01-1557/.

[21] von Heesen, W., and Höpfer, M., "Suppression of Wind Tunnel Buffeting by Active Flow Control," SAE International, 2004, pp. 2004–01–0805. https://doi.org/10.4271/2004-01-0805, URL https://www.sae.org/content/2004-01-0805/.

[22] Gomes, J. P., Bergmann, A., and Holthusen, H., "Aeroacoustic wind tunnel design," *CEAS Aeronaut J*, Vol. 10, No. 1, 2019, pp. 231–249. https://doi.org/10.1007/s13272-019-00372-7, URL http://link.springer.com/10.1007/s13272-019-00372-7.

[23] Fuchs, H. V., *Raum-Akustik und Lärm-Minderung: Konzepte mit innovativen Schallabsorbern und -dämpfern*, 4th ed., VDI-Buch, Springer Vieweg, Berlin, 2017. OCLC: 958465545.

[24] Duell, E. G., Kharazi, A., Muller, S., Ebeling, W., and Mercker, E., "The BMW AVZ Wind Tunnel Center," SAE International, 2010, pp. 2010–01–0118. https://doi.org/10.4271/2010-01-0118, URL https://www.sae.org/content/2010-01-0118/.

[25] McKillen, J., Walter, J., and Geslin, M., "The Honda R\&D Americas Scale Model Wind Tunnel," *SAE Int. J. Passeng. Cars - Mech. Syst.*, Vol. 5, No. 1, 2012, pp. 289–303. https://doi.org/10.4271/2012-01-0301, URL https://www.sae.org/content/2012-01-0301/.

[26] Fischer, O., *Investigation of Correction Methods for Interference Effects in Open-Jet Wind Tunnels*, 1st ed., Wissenschaftliche Reihe Fahrzeugtechnik Universität Stuttgart, Springer Fachmedien Wiesbaden : Imprint: Springer Vieweg, Wiesbaden, 2018. https://doi.org/10.1007/978-3-658-21379-4.

[27] Hennig, A., *Eine erweiterte Methode zur Korrektur von Interferenzeffekten in Freistrahlwindkanälen für Automobile*, Wissenschaftliche Reihe Fahrzeugtechnik Universität Stuttgart, Springer Vieweg, Wiesbaden [Heidelberg], 2017.

[28] Achzehnter, D., "Development and commissioning of a scale model of the ISTM closed circuit wind tunnel," Bachelor Thesis, Karlsruhe Institute of Technology, Karlsruhe, 2021.

[29] Romberg, G. F., Gunn, J. A., and Lutz, R. G., "The Chrysler 3/8-Scale Pilot Wind Tunnel," SAE International, 1994, p. 940416. https://doi.org/10.4271/940416, URL https://www.sae.org/content/940416/.

[30] Holthusen, H., and Kooi, J. W., "Model and full scale investigations of the low frequency vibration phenomena of the DNW open jet," *Agard Conference Proceedings*, Vol. 585, AGARD, Moscow, Russia, 1997, pp. 26–x.

[31] Walter, J., Duell, E., Martindale, B., Arnette, S., Geierman, R., Gleason, M., and Romberg, G., "The DaimlerChrysler Full-Scale Aeroacoustic Wind Tunnel," SAE International, 2003, pp. 2003–01–0426. https://doi.org/10.4271/2003-01-0426, URL https://www.sae.org/content/2003-01-0426/.

[32] Heuberger, A., and Gamm, E., *Software Defined Radio-Systeme für die Telemetrie: Aufbau und Funktionsweise von der Antenne bis zum Bit-Ausgang*, Springer Vieweg, Berlin; [Heidelberg], 2017. https://doi.org/10.1007/978-3-662-53234-8.

[33] Weiss, J., "A Tutorial on the Proper Orthogonal Decomposition," *AIAA Aviation 2019 Forum*, American Institute of Aeronautics and Astronautics, Dallas, Texas, 2019. https://doi.org/10.2514/6.2019-3333, URL https://arc.aiaa.org/doi/10.2514/6.2019-3333.

[34] Taira, K., Brunton, S. L., Dawson, S. T. M., Rowley, C. W., Colonius, T., McKeon, B. J., Schmidt, O. T., Gordeyev, S., Theofilis, V., and Ukeiley, L. S., "Modal Analysis of Fluid Flows: An Overview," *AIAA Journal*, Vol. 55, No. 12, 2017, pp. 4013–4041. https://doi.org/10.2514/1.J056060, URL https://arc.aiaa.org/doi/10.2514/1.J056060.

[35] Schmidt, O. T., and Colonius, T., "Guide to Spectral Proper Orthogonal Decomposition," *AIAA Journal*, Vol. 58, No. 3, 2020, pp. 1023–1033. https://doi.org/10.2514/1.J058809, URL https://arc.aiaa.org/doi/10.2514/1.J058809.

[36] Weber, K., "Development and Validation of a distributed Measurement System for a Modal Analysis of the "Göttinger Windkanal"," Master's thesis, Karlsruhe Institute of Technology, Karlsruhe, 2022.

[37] Elsner, F., "Testing of optimisation measures on the scale model of the closed return wind tunnel at ISTM," Bachelor Thesis, Karlsruhe Institute of Technology, Karlsruhe, 2022.

[38] Ochmann, R., and Peichl, A., *Measuring distributional effects of fiscal reforms*, No. Nr. 2006,9 in Finanzwissenschaftliche Diskussionsbeiträge, Finanzwiss. Forschungsinst, Köln, 2006.

[39] Kauffmann, F. J., "Testing of improvement measures at the nozzle outlet of the Göttinger wind tunnel at ISTM," Bachelor Thesis, Karlsruhe Institute of Technology, Karlsruhe, 2022.

[40] Anderson, A. B. C., "Structure and Velocity of the Periodic Vortex-Ring Flow Pattern of a *Primary Pfeifenton* (Pipe Tone) Jet," *The Journal of the Acoustical Society of America*, Vol. 27, No. 6, 1955, pp. 1048–1053. https://doi.org/10.1121/1.1908112, URL https://pubs.aip.org/asa/jasa/article/27/6/1048-1053/614393.

[41] Wickberg, M., "Investigation of collector improvement measures at the scale model of the Göttinger wind tunnel at ISTM," Bachelor Thesis, Karlsruhe Institute of Technology, Karlsruhe, 2022.

[42] Rufer, J., "Testing of two new collectors with breather gap to improve the flow at the closed-circuit wind tunnel at ISTM," Bachelor Thesis, Karlsruhe Institute of Technology, Karlsruhe, 2023.